

## Deformation analysis of high CFRD considering the scaling effects

Raksiri Sukkarak<sup>1</sup>, Pornthap Pramthawee<sup>1</sup>, Pornkasem Jongpradist<sup>\*1</sup>, Warat Kongkitkul<sup>1</sup>  
and Pitthaya Jamsawang<sup>2</sup>

<sup>1</sup>Department of Civil Engineering, King Mongkut's University of Technology Thonburi, ThungKhru, Bangkok, Thailand

<sup>2</sup>Department of Civil Engineering, Soil Engineering Research Center, King Mongkut's University of Technology North Bangkok, Bangkok, Thailand

(Received January 23, 2017, Revised May 12, 2017, Accepted July 13, 2017)

**Abstract.** In this paper, a predictive method accounting for the scaling effects of rockfill materials in the numerical deformation analysis of rockfill dams is developed. It aims to take into consideration the differences of engineering properties of rockfill materials between in situ and laboratory conditions in the deformation analysis. The developed method is based on the modification of model parameters used in the chosen material model, which is, in this study, an elasto-plastic model with double yield surfaces, i.e., the modified Hardening Soil model. Datasets of experimental tests are collected from previous studies, and a new dataset of the Nam Ngum 2 dam project for investigating the scaling effects of rockfill materials, including particle size, particle gradation and density, is obtained. To quantitatively consider the influence of particle gradation, the coarse-to-fine content (C/F) concept is proposed in this study. The simple relations between the model parameters and particle size, C/F and density are formulated, which enable us to predict the mechanical properties of prototype materials from laboratory tests. Subsequently, a 3D finite element analysis of the Nam Ngum 2 concrete face slab rockfill dam at the end of the construction stage is carried out using two sets of model parameters (1) based on the laboratory tests and (2) in accordance with the proposed method. Comparisons of the computed results with dam monitoring data indicate that the proposed method can provide a simple but effective framework to take account of the scaling effect in dam deformation analysis.

**Keywords:** scaling effects; modified model; coarse-to-fine content; finite element analysis; concrete face rockfill dam

### 1. Introduction

Concrete face slab rockfill dams (CFRDs) are increasingly constructed for many purposes, for instance irrigation, human consumption, flood control and hydropower. The settlements and horizontal movements are the main concerns in the design and operation of this dam type (Xu *et al.* 2012b). Large deformation of rockfill materials, which are the main material of this dam type, could induce abnormal behavior in the contact between the concrete face slabs and cushion layer or may cause cracks in the face slab (Cook 1984). It is thus important to accurately simulate the deformation of CFRD (Kim *et al.* 2014). At the present, numerical approach by the finite element method (FEM) or finite difference method (FDM) has mainly been used to analyze the behavior of CFRDs. One of the key points in the analysis is the determination of the model parameters to cooperate with the selected constitutive model for reproducing a reasonable response of the rockfill materials under loading.

The mechanical properties of rockfill materials are essentially determined from laboratory tests. In the laboratory, samples with maximum particle size in the range of 25-80 mm are typically prepared using one of the scaling techniques (i.e., parallel gradation technique, scalping

method, equivalent substitution method and combination method). In reality, the composition of rockfill material in a construction site is typically comprised of silt, gravel, cobbles, and boulders, which probably have maximum sizes of over 1 m in diameter (see Fig. 1). This scaling effect results in differences of the engineering properties of rockfill materials between in situ and laboratory conditions. To gain insights into this problem, the influence of particle size on the deviator stress-strain-volumetric strain behavior of rockfill materials has been experimentally examined by many investigators (e.g., Varadarajan *et al.* 2003 and 2006, Honkanadavar and Sharma 2014). Rockfill samples have been scaled down by using the parallel gradation method with maximum diameters of 25-80 mm. For quarried rockfills (used in most dams (Li *et al.* 2016)), the experimental results indicate that an increase of the particle size reduces the elastic stiffness and peak deviator stress, and more contraction behavior is observed. However, the scaling effects correspond to not only the effect of particle size but also the effect of particle gradation. A number of scientific papers related to the influence of particle gradation on the mechanical behaviors of rockfill materials have been published during the past decades (e.g., Kokusho *et al.* 2004, Hamidi *et al.* 2012, Tabibnejad *et al.* 2014). All of them reported experimental investigations on the influence of particle gradation of rockfill materials on the shear strength, deformation and collapse behaviors. The laboratory results indicated that the shear strength characteristics are enhanced with increasing gravel content.

\*Corresponding author, Associate Professor  
E-mail: [pornkasem.jon@kmutt.ac.th](mailto:pornkasem.jon@kmutt.ac.th)

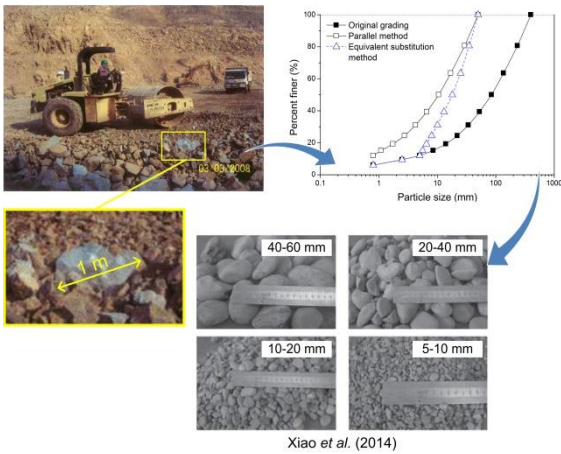
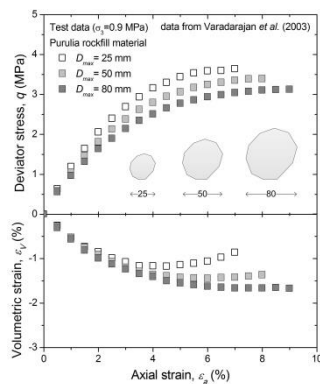
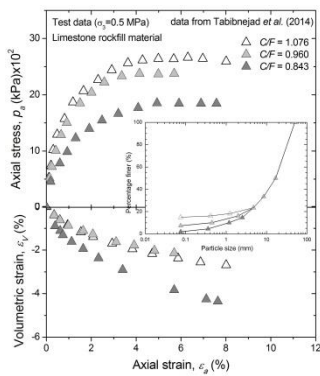


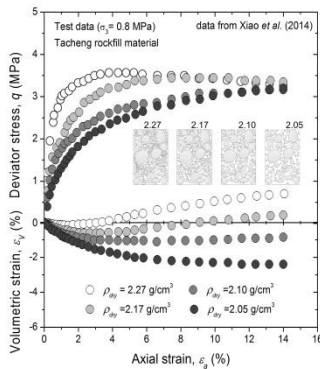
Fig. 1 The prototype rockfill used in dam construction and the scaled gradation used for laboratory samples



(a) particle size



(b) particle gradation



(c) density

Fig. 2 Stress-strain-volumetric strain behaviors of rockfill materials

Due to the realization of scaling effects on rockfill properties, preparing rockfill materials for testing with a smaller density of the prototype rockfill material is currently used in engineering practice (Xu *et al.* 2012a). In recent years, a series of large scale triaxial compression on Tacheng rockfill materials with different initial densities has been conducted by Xiao *et al.* (2014). For the specimen prepared with the highest density in the study, the material exhibits dilation behavior at the very beginning of shearing. The dilation behavior is gradually suppressed with diminished dry density. Although a number of research investigations have been conducted on the effects of different states between laboratory preparation and in situ conditions, each of them only focused on a certain factor (size or gradation or density).

Aside from experimental results, many investigators have attempted to develop constitutive models and numerical methods for simulating the response of triaxial test results (e.g., Varadarajan *et al.* 2003 and 2006, Zhang *et al.* 2007, Liu and Zou 2013, Ma *et al.* 2014, Pramthawee *et al.* 2017). The disturbed state concept developed by Desai (1995 and 2001) was used to investigate the effects of particle shape (round and angular shapes) and particle size (Varadarajan *et al.* 2003). A state-dependent model based on the critical state framework was developed to describe the behavior with different initial void ratios (Xiao *et al.* 2014). However, among the comprehensive studies related to scaling effects, most of them are still limited to the simulation of only the stress-strain relations of triaxial testing results.

In parallel, many finite element analysis applications in conjunction with back analysis methods have been carried out to investigate the field mechanical properties via case histories (e.g., Zhou *et al.* 2011, Wang *et al.* 2014, Jia and Chi 2015, Zhou *et al.* 2016). The hyperbolic elastic model developed by Duncan and Chang (1970) has been commonly utilized for simulating the triaxial stress-strain curves together with back-analysis methods, i.e., particle swarm optimization (Zhou *et al.* 2011), evolution algorithm (Yu *et al.* 2007), colony optimization (Kang *et al.* 2009) and clonal selection algorithm (Zheng *et al.*, 2013). Model parameters were computed by considering the dam deformation of the selected observation point. However, the model parameters obtained from the back-analysis method are not directly associated with the laboratory data. The computed model parameters, for instance  $K$  (modulus number),  $K_b$  (bulk modulus number) and  $n$  (exponential number) values, are strongly affected by each calculation method. The back-analysis methods also need enough monitoring data from several observation points to attain high validity.

Despite the fact that some attention has been paid to study the scaling effect of rockfill materials, there is still no link of such effect in dam deformation analysis. This current study intends to develop a method to take the scaling effect into account in dam deformation analysis by numerical simulation. The main concept is to modify the model parameters used in a chosen material model from the test state to the in-situ state. To achieve this, relations between key influencing factors and model parameters need to be established. A series of experimental data collected from the literature and a new dataset of Nam Ngum 2

(NN2) rockfill materials are used in this paper. The influence of particle size, particle gradation and density on the response of rockfill materials, as well as the strength, stiffness and volumetric strain, is discussed. To quantitatively take the influence of particle gradation into account, the coarse-to-fine content (C/F) concept is proposed in this study. In all numerical analyses, an elasto-plastic model with double yield surfaces, namely a modified hardening soil model (Sukkarak *et al.* 2017), is employed to characterize the response of rockfill materials. The three-dimensional (3D) FE analysis of NN2 CFRD during the construction stage is carried out using two sets of model parameters, i.e., (1) directly obtained from the calibration of laboratory tests and (2) using the established relations in this study to transform to in-situ conditions. Finally, the comprehensive dam monitoring data (including settlements, lateral movements toward upstream-downstream and longitudinal directions) are compared with the computed results to highlight the importance of scaling effects and to confirm the effectiveness of the developed method on the improvement of dam deformation analysis.

## 2. Concept, assumptions and limitations

### 2.1 General

This section describes briefly the impacts of key influencing factors, i.e., particle size, particle gradation and density on the behavior. On the basis of the problem stated previously, the developed method must be capable of characterizing the influence of not only the particle size but also the gradation on the parameters affecting the behavior of rockfills. Moreover, because a smaller density is commonly considered in current practice for the laboratory test as indicated by the available case studies (shown later), the influence of density is also included in the study. The coarse-to-fine content (C/F) (modified from Sánchez-Leal 2007) is proposed to quantitatively define a unique parameter representing the particle gradation. Subsequently, the relationships between the constitutive model parameters and key influencing factors are established as the simple functions.

*Particle size*-The experimental studies on the influence of particle size and particle shape have been investigated extensively in the literature (e.g., Marsal 1967, Marachi *et al.* 1969, Varadarajan *et al.* 2003 and 2006). In the experiments conducted by Varadarajan *et al.* (2003 and 2006), the specimens were prepared by using the parallel gradation technique (Lowe 1964) to scale the particle size. Fig. 2(a) shows the relationship from the drained triaxial test of Purulia rockfill material for tests with  $\sigma_3$  of 0.8 MPa (as an example). The elastic stiffness decreases with the maximum particle size. In the same manner, with full set of experimental results for various  $\sigma_3$ , the friction angle and dilation angle decrease with the maximum particle size. In term of the volumetric strain response, for quarried material, the rockfill achieving the largest deviator stress ( $D_{\max} = 25$  mm) exhibits the highest dilatancy.

*Particle gradation*-A further effect on the rockfill behavior is particle gradation (see Fig. 2(b)). A difference in particle gradation leads to changes in the mechanical behaviors of rockfill materials, as reported by a number of

researchers (Kokusho *et al.* 2004, Ramon *et al.* 2008, Hamidi 2012, Meng *et al.* 2014, Wei *et al.* 2014). More recently, Tabibnejad *et al.* (2014) showed that the stiffness modulus decreases with an increase of fine content. Consistent with other groups of researchers, they showed that the shear strength parameters increase with an increase of gravel content (Kokusho *et al.* 2004, Hamidi 2012, Tabibnejad *et al.* 2014, Meng *et al.* 2014).

*Density*-Concerning the effect of density, Xiao *et al.* (2014) performed a series of triaxial tests on Tacheng rockfill material with a wide range of initial density and pressure. Fig. 2(c) shows the triaxial test results at a confining pressure of 0.8 MPa of the specimens with different initial dry densities. As shown in the figure, the different initial dry densities have a significant effect on the response of rockfill material. The peak deviator stress and stiffness modulus increase with increasing dry density. For the highest density specimen, the material exhibits dilation behavior at the very beginning of shearing. The dilation behavior is gradually suppressed with diminished dry density.

In conclusion, the properties that depend on the particle size, particle gradation and density include the stiffness modulus, shear strength characteristic (commonly shown in terms of the friction angle) and dilatancy. Therefore, to reflect the deformation behavior, the favorable models must include these properties in the model parameters. These include most models in the family of elasto-plasticity, such as the generalized plastic model (Mroz and Zienkiewicz 1984) and hardening soil (HS) model (Schanz *et al.* 1999). In this study, a modified model (described later) based on the framework of the HS model is chosen. The stiffness modulus, shear strength characteristic and dilatancy are represented by  $E_{50}$  (together with  $E_{oed}$  and  $E_{ur}$ ),  $\phi$  and  $\psi$  respectively, in the HS model (see later for details).

As described above, each research in the past has focused only on a single influencing factor individually. Moreover, no sufficiently available information considering the effect of several influencing factors with the same type of rockfill exists; it is then difficult to characterize the effects of several influencing factors simultaneously on each property. In this study, each property is thus characterized by each influencing parameter separately to obtain a simple relationship. These relationships of each influencing parameter are later combined together to transform the parameters from the laboratory testing condition to the in-situ condition as shown in Eq. (1), assuming that no interaction exists among the factors.

$$A = A_0 \cdot F(D_{\max}, C/F, \rho_d) = A_0 \cdot F_1(D_{\max}) \cdot F_2(C/F) \cdot F_3(\rho_d) \quad (1)$$

where  $A$  represents each model parameter which shows a relationship against  $D_{\max}$ , particle gradation and dry density. Either a linear or power function is used for establishing the simple relation for parameter predictions. With a limited range of each influencing parameter in engineering practice, these two simple mathematical forms provide a sufficiently accurate characterization. The following power function form is considered in this study (see Fig. 3)

$$A = A_y (D_{\max})^\lambda \quad (2)$$

The parameters  $A_y$  and  $\lambda$  are constants in the power

function.

## 2.2 Coarse-to-fine content (C/F) concept

While the effect of the particle size and density can be quantitatively represented by the maximum particle size ( $D_{max}$ ) and dry density ( $\rho_d$ ) of the prepared rockfills, the gradation cannot be directly quantified as a single parameter. In this study, a similar concept from research on mixed asphalt is adopted. A convenient form, i.e., Gravel-to-Sand (G/S) (Sánchez-Leal 2007), has been used to study the performance (i.e., workability, resistance to rutting and permeability) of mixed asphalt materials with different particle gradations. For that purpose, there are two parameters, i.e.,  $D_{max}$  and  $n$ . The parameter  $n$  is the shape coefficient and  $D_{max}$  is the maximum particle size, which must be obtained from the gradation curve. To reliably obtain the parameter  $n$ , the Fuller's model is recommended (Sánchez-Leal 2007).

The definition of gravel content ( $G$ ) can be expressed as

$$G = 1 - p_{4.75} \quad (3)$$

where  $p_{4.75}$  defines the percentage finer than No. 4 (4.75 mm). The fine content ( $F$ ) is written as follows

$$F = p_{0.075} \quad (4)$$

Sand content ( $S$ ) is limited by

$$S = 1 - (1 - p_{4.75}) - p_{0.075} = p_{4.75} - p_{0.075} \quad (5)$$

Consequently, a general expression can be inferred for any combinations of gravel  $G$  and sand  $S$  contents (see Fig. 4(a)) by dividing Eq. (3) by Eq. (5) as follows

$$\frac{G}{S} = \frac{D_{max}^n - 4.75^n}{4.75^n - 0.075^n} \quad (6)$$

As suggested by Sánchez-Leal, we notice that the range of gravel content used in pavement works is obviously smaller than that of the rockfill material applications. Therefore, the original concept of G/S is modified in this study markedly as Course-to-Fine (C/F) (see Fig. 4(b)). The coarse content is given by

$$C = 1 - p_{D_{50}} \quad (7)$$

The fine content ( $F$ ) is given by

$$F = p_{D_{50}} - p_{D_{min}} \quad (8)$$

A general expression can be inferred for any combinations of coarse  $C$  and fine  $F$  contents by dividing Eq. (7) by Eq. (8), as follows

$$C / F = \frac{D_{max}^n - D_{50}^n}{D_{50}^n - D_{min}^n} \quad (9)$$

The effectiveness of this proposed C/F is that it is adaptable for a wide range of particle sizes. In case that the material is scaled down by using the parallel gradation technique, the ratio of C/F does not change.

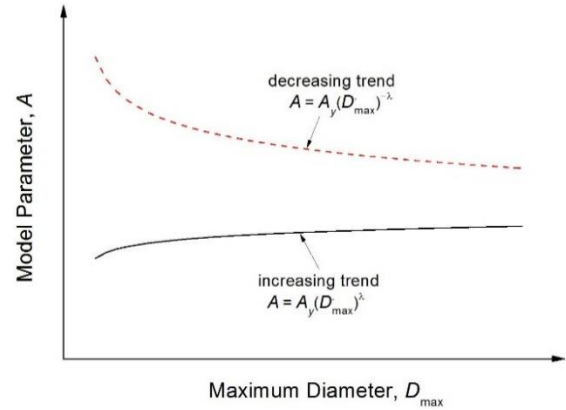


Fig. 3 Power functions used in the model parameter calculations for rockfill materials

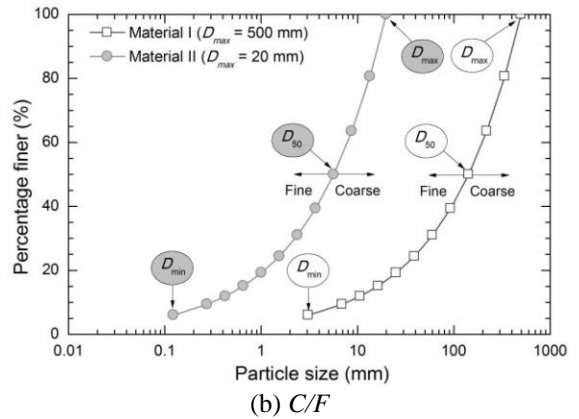
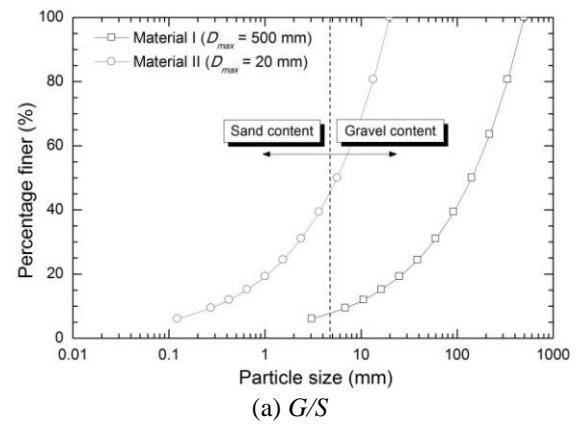


Fig. 4 Graphical representation of classification

## 3. Constitutive model and determination of parameters

The modified hardening soil (HS) model (Sukkarak *et al.* 2017) in the family of elasto-plasticity (originally developed for fine grained soils i.e., sands and clays (Schanz *et al.* 1999) and later modified for rockfill materials) has been chosen in this study. The original model (hardening soil model) has been extensively used in numerical analyses of various kinds of geotechnical works (e.g., Pramthawee *et al.* 2011, Jongpradist *et al.* 2013, Chen *et al.* 2014, Hosseinzadeh and Joosse 2015, Jamsawang *et al.* 2016). The salient features of the model are briefly

described herein.

First, a number of large-scale triaxial experiments have illustrated that the friction angle of a rockfill material is a function of the confining pressure. Thus, the friction angle of the modified model can be obtained as

$$\varphi = \varphi_0 - \Delta\varphi \log\left(\frac{\sigma'_3}{p_a}\right) \quad (10)$$

where  $p_a$  is the atmospheric pressure,  $\varphi_0$  is the reference friction angle, and  $\Delta\varphi$  is the reduction factor. According to the hyperbolic model developed by Duncan and Chang (1970), a principle hyperbolic function is used to express the stress-strain relations of the current model in primary triaxial loading. Here,  $\varepsilon_1$  is the vertical strain and  $q$  is the deviator stress. Based on the standard drained triaxial tests, the relationship between  $\varepsilon_1$  and  $q$  can be expressed as

$$-\varepsilon_1 = \frac{1}{E_i} \frac{q}{1 - q/q_a} \text{ for } : q < q_f \quad (11)$$

where  $q_a$  and  $E_i$  are the asymptotic value and the initial stiffness.

For yield surfaces, the shear hardening yield function  $f$  has been specified in the following form

$$f = \bar{f} - \gamma^p \quad (12)$$

$$\bar{f} = \frac{2}{E_i} \frac{q}{1 - q/q_a} - \frac{2q}{E_w} \quad (13)$$

$$\gamma^p = -(2\varepsilon_1^p - \varepsilon_v^p) \approx -2\varepsilon_1^p \quad (14)$$

Here,  $\bar{f}$  and  $\gamma^p$  are the function of stress and plastic strains respectively. The second yield function for the yield cap is expressed as follows

$$f^c = \frac{\tilde{q}^2}{\alpha^2} + p'^2 - p_p^2 \quad (15)$$

where  $\tilde{q}$  is a special stress measure for deviatoric stresses and  $\alpha$  is an auxiliary model parameter that is related to  $K_0^{nc}$ . For an associated flow rule in plasticity, plastic potential function  $g^c$  is defined as the same of a yield function  $f^c$  by

$$g^c = f^c \quad (16)$$

The actual stiffness modulus are updated according to current stress level which controlled by the model constant (power parameter). Based on previously studied (Sukkarak *et al.* 2017), the power parameters in the stress states corresponding to triaxial and oedometer tests were defined separately and denoted by  $m$  and  $n$  for triaxial and oedometer tests, respectively

$$E_{50} = E_{50}^{ref} \left( \frac{c \cos \varphi - \sigma'_3 \sin \varphi}{c \cos \varphi + p^{ref} \sin \varphi} \right)^m \quad (17)$$

$$E_{oed} = E_{oed}^{ref} \left( \frac{c \cos \varphi - \sigma'_3 / K_0^{nc} \sin \varphi}{c \cos \varphi + p^{ref} \sin \varphi} \right)^n \quad (18)$$

Table 1 Experimental data used in this study

| Source      | Materials                | $D_{max}$ (mm) | $P_d$ ( $g/cm^3$ )    | Variation of test specimen |       |     | Reference                        |
|-------------|--------------------------|----------------|-----------------------|----------------------------|-------|-----|----------------------------------|
|             |                          |                |                       | $D_{max}$                  | $P_d$ | GSD |                                  |
| Kol dam     | Limestone                | 25,50,80       | NIA                   | √                          |       |     | Varadarajan <i>et al.</i> (2006) |
| Purulia dam | Hornblende-quartz-schist | 25,50,80       | NIA                   | √                          |       |     | Varadarajan <i>et al.</i> (2006) |
| Parbati dam | Quartzite                | 20,40,80       | NIA                   | √                          |       |     | Varadarajan <i>et al.</i> (2006) |
| Tacheng     | Granite, conglomerate    | 60             | 2.05, 2.102, 17, 2.27 |                            | √     |     | Xiao <i>et al.</i> (2014)        |
| NIA         | Limestone                | 50             | 2.15                  |                            |       | √   | Tabibnejad <i>et al.</i> (2014)  |

NIA: No Information Available, GSD: Grain Size Distribution

The stress-dependent stiffness modulus in cases of unloading and reloading stress paths can be expressed as

$$E_{ur} = E_{ur}^{ref} \left( \frac{c \cos \varphi - \sigma'_3 \sin \varphi}{c \cos \varphi + p^{ref} \sin \varphi} \right)^m \quad (19)$$

According to the original Rowe's stress-dilatancy theory, the dilatancy equation can be written as follows

$$\sin \psi_m = \frac{\sin \varphi_m - \sin \varphi_{cv}}{1 - \sin \varphi_m \sin \varphi_{cv}} \quad (20)$$

where  $\psi_m$  is the mobilized dilatancy angle and  $\varphi_{cv}$  and  $\varphi_m$  are the critical state friction angle and mobilized friction angle, respectively.

#### 4. Investigation with existing experimental data

In the current study, the datasets of experimental tests for various particle sizes, particle gradations and dry densities were collected from previous studies (Varadarajan *et al.* 2003 and 2006, Xiao *et al.* 2014, Tabibnejad *et al.* 2014) and a new dataset of the Nam Ngum 2 dam project. The relationships of rockfill material factors (particle size, particle gradation and density) with the constitutive model parameters are established. Detailed information of the experimental data is illustrated in Table 1. The constitutive model parameters ( $\varphi_0$ ,  $\psi$  and  $E_{50}^{ref}$ ) were directly determined from the test results.

##### 4.1 Characterization of particle size on model parameter

The effect of the particle size is observed in the case of test samples prepared with the parallel gradation method (C/F constant-no influence of particle gradation). The friction angle decreases logarithmically as the maximum diameter increases. Similar relationships are also found for the different sources of rockfill materials. To investigate the influence of particle size on the mechanical response of rockfill materials, Figs. 5(a)-5(c) show the dependencies of  $\varphi_0$ ,  $\psi$  and  $E_{50}^{ref}$  on  $D_{max}$ , together with the regression, by power relationships in the forms of

$$\varphi_0 = \varphi_y (D_{max})^{\lambda_1} \quad (21)$$

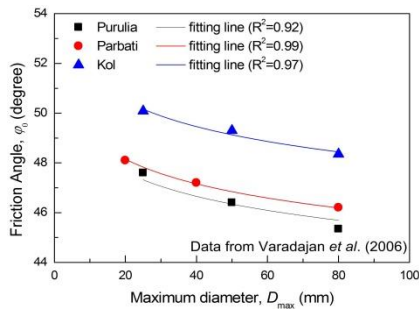
$$\psi = \psi_y (D_{max})^{\lambda_2} \quad (22)$$

$$E_{50}^{ref} = E_{50,y}^{ref} (D_{max})^{\lambda_3} \quad (23)$$

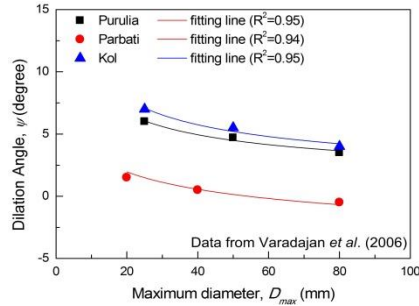
where  $\varphi_y$ ,  $\psi_y$  and  $E_{50,y}^{ref}$  are the material constants;  $\lambda_1$ ,  $\lambda_2$  and  $\lambda_3$  are the power law constants. It is seen that the coefficients of determination  $R^2$  of the regression results of all parameters are higher than 0.92, except for  $E_{50}^{ref}$  of Kol rockfill. These correlations enable the prediction of model parameters for various particle sizes. An interesting observation is that the  $\lambda$  values vary within a small range; it may thus be applicable to impose  $\lambda$  as a constant.

4.2 Characterization of particle gradation on model parameter

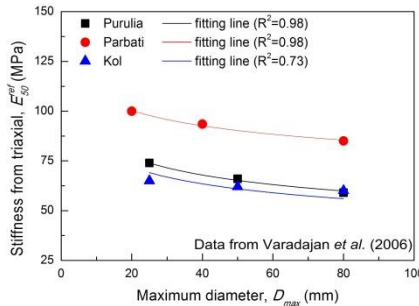
According to several existing scaling techniques, e.g., parallel gradation technique, scalping method, equivalent substitution method and combination method, the influence of particle gradation can be very significant in the design of mixtures of test materials. Fig. 6(a) illustrates the gradation curves used in the experimental work of Tabibnejad *et al.* (2014). Three samples were prepared with different gradations. Fig. 6(b) presents, for instance, the fitting of the gradation of rockfill with 2% fine content by Fuller’s model



(a) friction angle

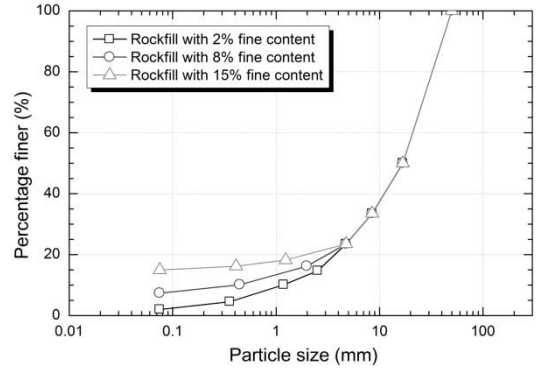


(b) dilation angle

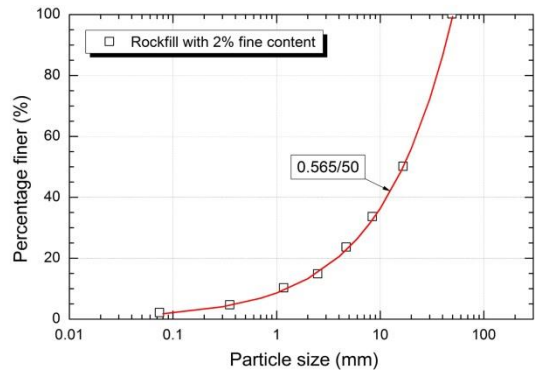


(c) stiffness modulus from triaxial test

Fig. 5 Variation of model parameters with the particle size



(a) Grain size distribution for rockfill materials



(b) Allometric of Fuller’s model fit for data

Fig. 6 The gradation curves of rockfill materials used in this study

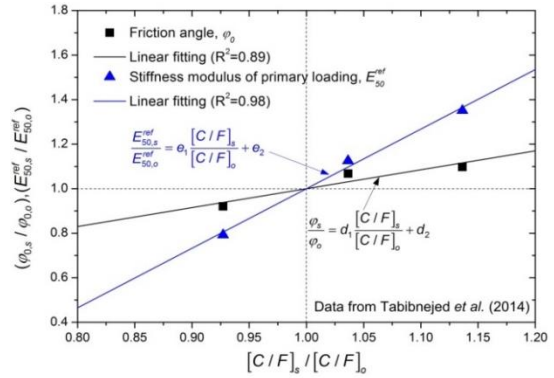
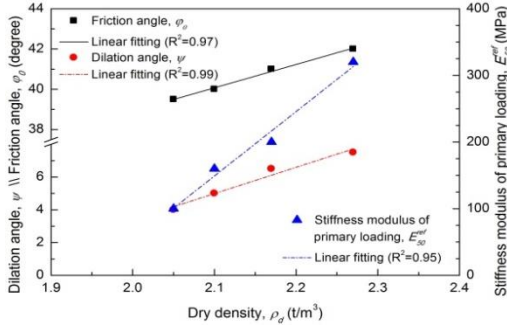


Fig. 7 Variation of model parameters with  $C/F$

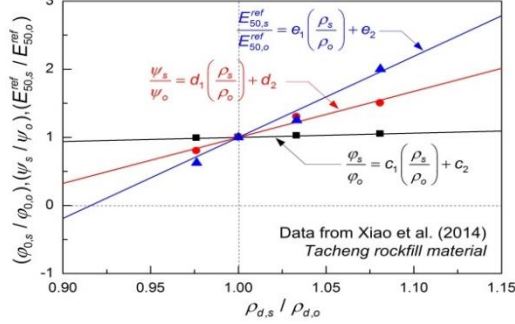
to obtain the parameters  $n$  and  $D_{max}$ . Note that Fuller’s model is used to quantify the curve of particle gradation (Sánchez-Leal 2007). The result indicates  $n = 0.565$  and  $D_{max} = 50$ .

As Tabibnejad *et al.* (2014) reported in their research findings, the shear strength and stiffness of rockfill materials increase as the fine content decreases (higher coarse content), and the difference of the dilation behavior is relatively small. Therefore, only  $\varphi$  and  $E_{50}^{ref}$  (determined from the test result) are considered to be influenced by the particle gradation.

Fig. 7 presents the influence of  $C/F$  on  $\varphi_0$  and  $E_{50}^{ref}$ , where  $[C/F]_o$  is a normalizing constant or original gradation,  $[C/F]_s$  is the scaled gradation, and  $\varphi_{0,o}$  and

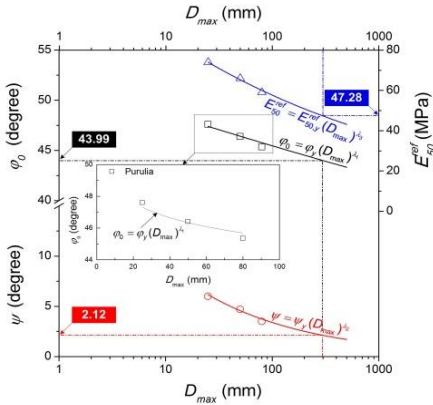
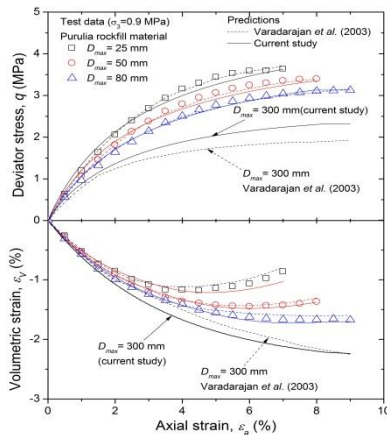


(a) Variation of model parameters with dry density



(b) Normalized of model parameters with dry density

Fig. 8 Fitting to testing data for different dry density of Tacheng rockfill material


 (a) Model parameters-in  $D_{max}$  for Purulia rockfill material


(b) Comparisons between simulation and test data from Purulia rockfill material

Fig. 9 Prediction of model parameters and stress-strain relationship

$E_{50,o}^{ref}$  are the normalizing constants at the original gradation. The parameters  $\varphi_{0,o}$  and  $E_{50}^{ref}$  increase with the  $C/F$  and can be approximated as

$$\frac{\varphi_{0,s}}{\varphi_{0,o}} = a_1 \left( \frac{[C/F]_s}{[C/F]_o} \right) + a_2 \quad (24)$$

$$\frac{E_{50,s}^{ref}}{E_{50,o}^{ref}} = b_1 \left( \frac{[C/F]_s}{[C/F]_o} \right) + b_2 \quad (25)$$

As mentioned earlier, if the material is scaled down by using the parallel gradation technique ( $C/F$  constant),  $\varphi_0$  and  $E_{50}^{ref}$  can be obtained without considering the particle gradation effect; however, consideration of the  $D_{max}$  effect still remains.

#### 4.3 Characterization of density on model parameters

Comprehensive experimental data focusing on the effect of density were obtained by Xiao *et al.* (2014). Tacheng rockfill material with various initial dry densities ( $\rho_d$ ) of 2.05-2.27  $t/m^3$  was tested with confining pressures of 0.4-1.6 MPa. Fig. 8(a) shows the variations of the model parameters with different dry densities. Their results indicated that the peak deviator stress and stiffness modulus increase with increasing dry density. Rockfill shows a contractive behavior when the dry density decreases.  $\varphi_p$ ,  $\psi$  and  $E_{50}^{ref}$  increase with increasing  $\rho_d$ . It is also observed that the values of  $\varphi_p$ ,  $\psi$  and  $E_{50}^{ref}$  show a linear increasing trend with  $\rho_d$ . In engineering practice, the dry density of the rockfill does not vary much and is typically in the range of 2.05-2.25  $t/m^3$ . This narrow range can be satisfactorily captured by a linear function. Fig. 8(b) presents the relationships between the normalized  $\varphi_p$ ,  $\psi$  and  $E_{50}^{ref}$  against the normalized  $\rho_d$ , where  $\rho_{d,o}$  is a normalizing constant or original dry density (taken to be 2.1  $t/m^3$ ),  $\rho_{d,s}$  is the considered dry density, while  $\varphi_0$ ,  $\psi_0$  and  $E_{50,o}^{ref}$  are the corresponding values at the original dry density. The density-dependent parameters can be expressed as

$$\frac{\varphi_{p,s}}{\varphi_{p,o}} = c_1 \left( \frac{\rho_{d,s}}{\rho_{d,o}} \right) + c_2 \quad (26)$$

$$\frac{\psi_s}{\psi_o} = d_1 \left( \frac{\rho_{d,s}}{\rho_{d,o}} \right) + d_2 \quad (27)$$

$$\frac{E_{50,s}^{ref}}{E_{50,o}^{ref}} = e_1 \left( \frac{\rho_{d,s}}{\rho_{d,o}} \right) + e_2 \quad (28)$$

where  $c_1$ ,  $c_2$ ,  $d_1$ ,  $d_2$ ,  $e_1$  and  $e_2$  are the constant values.

In conclusion, the model parameters (of the selected modified HS model) directly calibrated from tested rockfills with various  $D_{max}$ , gradation and density for all collected rockfill materials are carefully observed. The following conclusions are drawn:

- The investigation indicates the effect of the particle size, particle gradation and density on three independent model parameters, i.e.,  $\varphi_0$ ,  $\psi$  and  $E_{50}^{ref}$  ( $E_{oed}^{ref}$  and  $E_{ur}^{ref}$  are considered to be ratios of  $E_{50}^{ref}$ ).

- A strategy for transforming model parameters associated with scaling effects is provided in this section.

Note that particle breakage is not considered in this study. Based on previous studies, the behaviors of quarried and alluvial rockfills are different. In this study, only quarried rockfill, which is the main type of material for dam construction, is considered. However, the procedure proposed in this study can be extended for alluvial rockfills as well. Since a series of experimental data collected from several data sets, in order to enhance the reliability of the proposed method, future clarification should be done from series of tests on the same rockfill material.

**5. Prediction of model parameters and stress-strain relationship for prototype rockfills**

By using the developed method, different sets of parameters for different rockfills (different maximum sizes, densities and gradations) can be obtained. Table 2 provides the equations to calculate the transformed model parameters considering scaling effects. These model parameters were obtained by calibrating with the available triaxial test data from previous study.

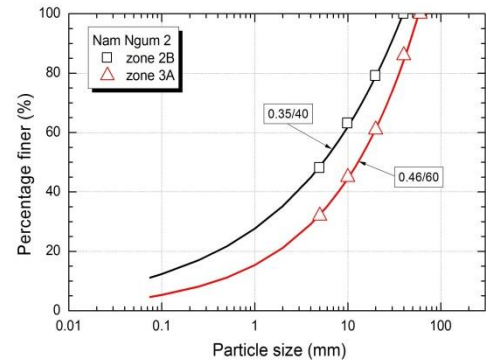
To examine the predictive ability of the method on model parameters, the simulations of  $q-\varepsilon_a-\varepsilon_v$  curves by the modified HS model with sets of parameters are performed. The simulation results are compared with those of the experiments. Fig. 9(a) shows the model parameters- $D_{max}$  relations of Purulia rockfill materials (with sizes in actual laboratory tests) in semi-logarithmic space together with the lines from obtained empirical equations (Eqs. (21)-(23)). The calculation of model parameters at  $D_{max}=300$  mm is also conducted by interpolating from the equations as shown in the figure. The simulation results considering the effect of particle size are presented in Fig. 9(b).

In the figure, the predicted  $q-\varepsilon_a-\varepsilon_v$  curves using the modified HS model with sets of parameters from both direct calibration of the test experiments (for  $D_{max}$  of 25, 50 and 80 mm) and calculated ones (from Fig. 9 for  $D_{max}$  of 300 mm) are compared with the actual testing data. Simulations using the model developed by Varadarajan *et al.* (2003) are also illustrated. The simulation results in this study are in good agreement with the tested data for various sizes of rockfills and found to be close to the predicted lines of Varadarajan *et al.* (2003), although small differences can be noticed. For the prediction of  $q-\varepsilon_a-\varepsilon_v$  curves of rockfill with  $D_{max}$  of 300 mm, the simulated result in this study exhibits lower stiffness and higher contraction compared to the results of smaller size rockfills. The result is also consistent and close to that of Varadarajan *et al.* (2003), although a little higher stiffness and contraction can be captured. The developed method can be used to transform the model parameters to provide satisfactory  $q-\varepsilon_a-\varepsilon_v$  response of prototype rockfill material.

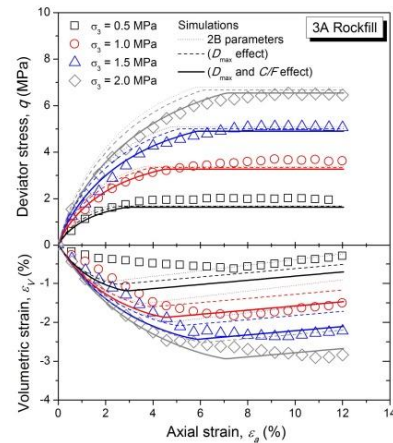
The data of laboratory tests on two sandstones (zone 2B and 3A) of the Nam Ngum 2 CFRD project conducted by the Institute of Water Resources and Hydropower Research (IWHR 2007) are used to validate the introduced concept of  $C/F$ . Fig. 10(a) shows the particle gradation distributions of materials 2B and 3A in laboratory testing, with  $D_{max}$

Table 2 Determination of scaling model parameters

| Case      | Formula  | Parameters used  |
|-----------|--|--|
| $D_{max}$ | $\varphi = \varphi_0 (D_{max})^{\lambda_1}, \psi = \psi_0 (D_{max})^{\lambda_2}$<br>$E_{50}^{ref} = E_{50,0}^{ref} (D_{max})^{\lambda_3}$  | $\lambda_1 = 0.037, \lambda_2 = 0.18, \lambda_3 = 0.18$<br>$\varphi_0, \psi_0, E_{50,0}^{ref} \rightarrow$ see Fig. 9(a) |
| GSD       | $\frac{\varphi_{0,s}}{\varphi_{0,o}} = a_1 \left( \frac{[C/F]_s}{[C/F]_o} \right) + a_2$<br>$\frac{E_{50,s}^{ref}}{E_{50,o}^{ref}} = b_1 \left( \frac{[C/F]_s}{[C/F]_o} \right) + b_2$   | $a_1 = 1.802, a_2 = -0.802$<br>$b_1 = 2.560, b_2 = -1.560$   |
| $\rho_d$  | $\frac{\varphi_{p,s}}{\varphi_{p,o}} = c_1 \left( \frac{\rho_{d,s}}{\rho_{d,o}} \right) + c_2, \frac{\psi_s}{\psi_o} = d_1 \left( \frac{\rho_{d,s}}{\rho_{d,o}} \right) + d_2$<br>$\frac{E_{50,s}^{ref}}{E_{50,o}^{ref}} = e_1 \left( \frac{\rho_{d,s}}{\rho_{d,o}} \right) + e_2$ | $c_1 = 0.609, c_2 = 0.391$<br>$d_1 = 6.737, d_2 = -5.734$<br>$e_1 = 12.682, e_2 = -11.748$                               |



(a) Allometric of Fuller's model fit for data



(b) Comparisons between simulation and experimental data

Fig. 10 Calibrating the prediction method with the available triaxial test results

Table 3 Model parameters used for Nam Ngum 2 CFRD

| Zone   | Parameter | $\varphi_0$ (deg.) | $\psi_0$ (deg.) | $E_{50,0}^{ref}$ (MPa) | $E_{over}^{ref}$ (MPa) | $m$  | $n$  | $\Delta\varphi$ | $R_f$ |
|--------|-----------|--------------------|-----------------|------------------------|------------------------|------|------|-----------------|-------|
| 2B     | Test      | 42.23              | 3.2             | 65.0                   |                        |      |      |                 |       |
|        | Scaling   | 41.84              | 3.16            | 84.3                   | $0.769E_{50}^{ref}$    | 0.45 | 0.25 | 1.16            | 0.74  |
|        | Change, % | -0.9               | -1.3            | -10.3                  |                        |      |      |                 |       |
| 3A     | Test      | 46.08              | 3.2             | 65.0                   |                        |      |      |                 |       |
|        | Scaling   | 43.66              | 2.55            | 56.9                   | $0.8E_{50}^{ref}$      | 0.34 | 0.22 | 2.59            | 0.75  |
|        | Change, % | -5.25              | -20.3           | -12.5                  |                        |      |      |                 |       |
| 3B1&3D | Test      | 47.09              | 3.2             | 80.0                   |                        |      |      |                 |       |
|        | Scaling   | 43.03              | 2.13            | 52.0                   | $0.688E_{50}^{ref}$    | 0.29 | 0.15 | 2.99            | 0.78  |
|        | Change, % | -8.26              | -33.4           | -35                    |                        |      |      |                 |       |
| 3B2    | Test      | 42.60              | 0.5             | 32.0                   |                        |      |      |                 |       |
|        | Scaling   | 38.93              | 0.13            | 20.8                   | $0.75E_{50}^{ref}$     | 0.69 | 0.35 | 2.55            | 0.82  |
|        | Change, % | -8.62              | -74             | -35                    |                        |      |      |                 |       |
| 3C1&3E | Test      | 42.00              | -5              | 20.0                   |                        |      |      |                 |       |
|        | Scaling   | 37.81              | -3.64           | 16.4                   | $0.85E_{50}^{ref}$     | 0.64 | 0.25 | 2.45            | 0.68  |
|        | Change, % | -9.98              | -27.2           | -18                    |                        |      |      |                 |       |
| 3C2    | Test      | 43.30              | -5              | 12.0                   |                        |      |      |                 |       |
|        | Scaling   | 38.98              | -3.64           | 9.8                    | $0.833E_{50}^{ref}$    | 0.70 | 0.22 | 3.95            | 0.65  |
|        | Change, % | -7.67              | -27.2           | -18.3                  |                        |      |      |                 |       |

$$E_w^{ref} = 3E_{50}^{ref}, p^{ref} = 100 \text{ kPa}, c = 1 \text{ kPa}, OCR = 1, K_0^{bc} = 1 - \sin \varphi, \nu_w = 0.3$$

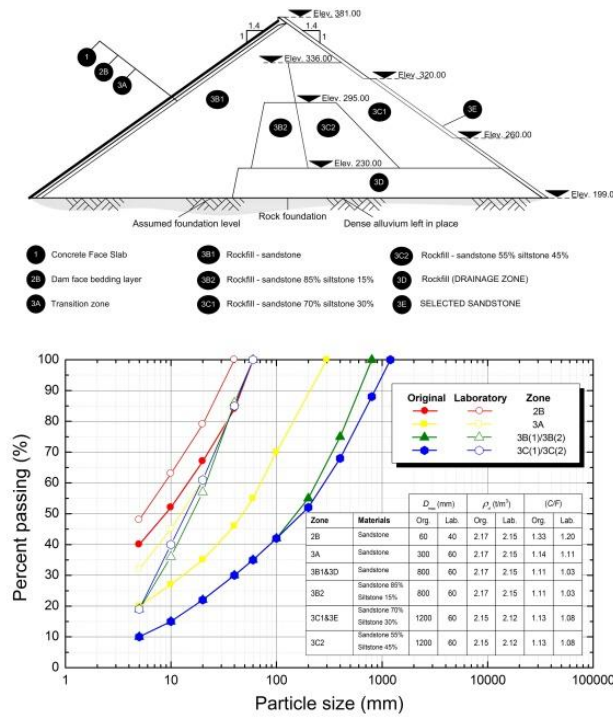


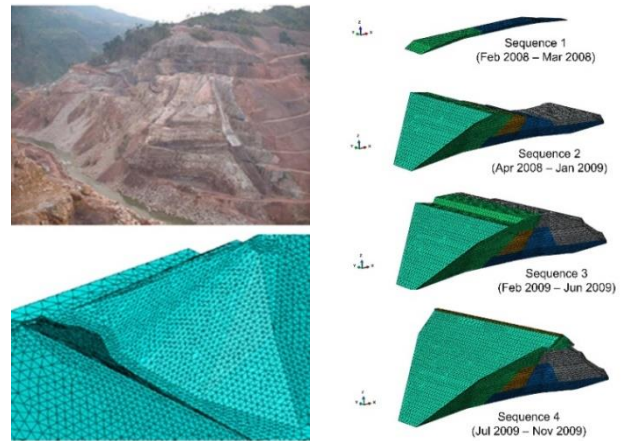
Fig. 11 Material zones of Nam Ngum 2 CFRD

of 40 and 60 mm, respectively. Material 2B is considered to be the prototype material, whereas material 3A is used as the prediction case. The model parameters were originally calibrated with the experimental data of the 2B rockfill. By using the developed relationships which account for the influences of particle size (Eqs. (21)-(23)) and particle gradation (Eqs. (24)-(25)), the parameters and, consequently, the  $q-\varepsilon_a-\varepsilon_v$  responses of 3A rockfill are predicted.

In Fig. 10(b), the thin dotted lines show the simulations using directly obtained parameters (from 2B rockfill). We first consider only the effect of particle gradation. The simulations using parameters obtained from the substitution of 2B rockfill parameters into Eqs. (21)-(23) are illustrated as thick dotted lines in the figure. The results show that only a small variation of the  $q-\varepsilon_a-\varepsilon_v$  response is observed, probably because the maximum sizes of these two rockfills are not much different. Next, the model parameters are transformed in conjunction with the introduced concept of  $C/F$  using Eqs. (24)-(25). The simulations using this set of parameters are represented in the figure as thick solid line. It can be seen that the simulation results become significantly different from the original ones (using 2B rockfill parameters), indicating the impact of particle gradation on rockfill response. By comparing the simulated results for the 3A rockfill (using transformed parameters) with real test data (depicted by symbols in the figure), good agreement on not only the stiffness but also the peak deviator stress and dilation angle after peak failure can be seen.

### 6. Case study of dam construction

The Nam Ngum 2 (NN2) CFRD project is located on the Nam Ngum river in Lao People’s Democratic Republic,



(a) Photo of valley and FE (b) FE stage of construction modeling

Fig. 12 3D FE simulation

approximately 90 km north of the capital Vientiane and 35 km upstream of the Nam Ngum 1 dam and powerhouse. The dam has a height of 182 m and crest length of 500 m. The dam volume is approximately 10 million m<sup>3</sup>, and the face slab area is approximately 88,000 m<sup>2</sup>. The designation of the CFRD rockfill zones follows the guidelines of the International Commission on Large Dams (ICOLD 2004). The dam has an upstream slope of 1V:1.4H (vertical: horizontal) and downstream slope of 1V:1.4H between two berms (slope 1V : 1.5H including berms). Fig. 11 displays a typical dam section of NN2 dam and the gradation curves of the test samples and the in situ approximate target grain size. In the preparation stage, a combination of the Equivalent Quantity Replacement Method (EQRM) and Similar Particle Distribution Method (SPDM) was performed to scale the materials down, in accordance to the

Specification of Soil Test of SL237-1999 (NJHRI 1999). The rockfill samples were prepared by controlling the compaction to obtain a dry unit weight of 2.10-2.15 t/m<sup>3</sup>, while the dry unit weight achieved for in situ compacted rockfill materials is greater than 2.15 t/m<sup>3</sup>. In assessing the quality of compacted materials, a number of field density tests

In this study, Hydrostatic settlement cells (HSC) and settlement gauges (SG) were installed to observe the internal settlement of the dam body. The lateral displacement (upstream-downstream and longitudinal directions) was monitored by Probe Inclinometers (PI). The PI and SG sets were installed at the identical location. The measured results are cumulative values after installation, except for the PI sets which were set to zero when the dam embankment level rose up to 140 m.

## 7. Finite element analysis

The finite element software ABAQUS was employed to simulate the deformation response of NN2 CFRD. Fig. 12(a) presents the photo of the valley and FE modeling. Fig. 12(b) illustrates the 3D FE mesh of the dam body part during the stage of construction. The dam body and abutment/foundation were modeled by 4-node solid elements (C3D4), while the face slab was modeled by 3-node shell elements (S3). The modified HS model was numerically implemented into the FE program ABAQUS through user-defined subroutines. The model parameters used are listed in Table 3. The first set of parameters was directly calibrated from the triaxial test results, whereas another set was determined considering the scaling effects. The rock foundation/abutment was modeled as linear elastic properties with the typical characteristics of  $E=5$  GPa and  $\nu=0.2$ . The modulus of elasticity for the concrete is 20 GPa and poisson's ratio is 0.2. In the construction stage, gravity load was applied as the body force.

The interface between the dam body and face slab is considered in terms of interactions in normal and tangent directions. The sticking condition is assumed in the initial condition for both normal and tangential directions. In the normal direction, the behavior is treated as open under tension. If the shear stress in the tangential direction of the interface exceeds the shear strength of the interface, sliding between the two surfaces occurs (Tunsakul *et al.* 2013). It is also assumed that failure occurs when the shear stress along the predicted failure surface exceeds the Mohr-Coulomb shear strength as expressed in Eq. (29).

$$\tau > C + \sigma_n \times \tan \phi \quad (29)$$

Once the stress state attains the failure criterion, slip starts and the cohesion becomes zero. The post-failure behavior of the interface is then assumed to follow the Coulomb law

$$\tau > C + \sigma_n \times \tan \phi \quad (30)$$

The interface parameters followed a recent study on the interface between concrete slab and cushion layer of Sanbanxi CFRD (Zhang and Zhang 2008). A friction angle of 40 degrees was adopted, and the cohesion parameter of 0.5 MPa was assumed in this study. Perfect bonding (no slip condition) is assumed between the dam body and

abutment/foundation.

## 8. Results and discussion

Fig. 13 shows the computed deformation contours (section 3) using the laboratory parameter set (LP) and the scaling parameter set (SP), respectively.

The deformation trends of the computed results with LP and SP are similar. In terms of the deformation magnitude, the computed results with LP have smaller magnitudes than the results with SP. The maximum horizontal displacement along the upstream-downstream direction ( $u_x$ ) occurs at the middle dam height for both upstream and downstream sides. The horizontal displacement towards the upstream side is directed upstream. In contrast, the horizontal displacement towards downstream side is directed in the opposite direction. For the displacement along the longitudinal direction ( $u_y$ ), the dam body moves to the river for both left and right abutments. On section 3 (at river), the dam body exhibits only a few millimeters of horizontal displacement. In the case of dam settlement ( $u_z$ ), the maximum settlement occurs at the rockfill in zones 3C1 and 3C2 (slightly downstream) because the overall stiffness of these zones is lower than those of other zones. Based on the monitoring data, the ratio of the maximum settlement to dam height is 1.15%, which is very close to that of the dams having similar heights, i.e., Pubugou (186 m) and Maoergai (146 m).

Fig. 14 shows the comparison between the computed settlement and the monitoring data observed by the HSC sets. It can be immediately seen that the computed settlements with SP achieve a satisfactory match with the monitoring data in terms of the magnitude values and settlement trend. The computed settlements with LP are relatively smaller in magnitude, which is in agreement with the previous studies (e.g., Zhou *et al.* 2011, Jia and Chi 2015). The settlements at various elevations were observed by the Settlement Gauge (SG) sets located at the downstream zone. Fig. 15(a) shows the computed settlements and monitoring data of the SG set. It reveals that both computed results (LP and SP) are close to each other, particularly for sections 2 and 4 (SG 2.1 and SG 4.1), whereas slightly higher settlements can be seen at section 3 (SG 3.1) for the computed results by SP.

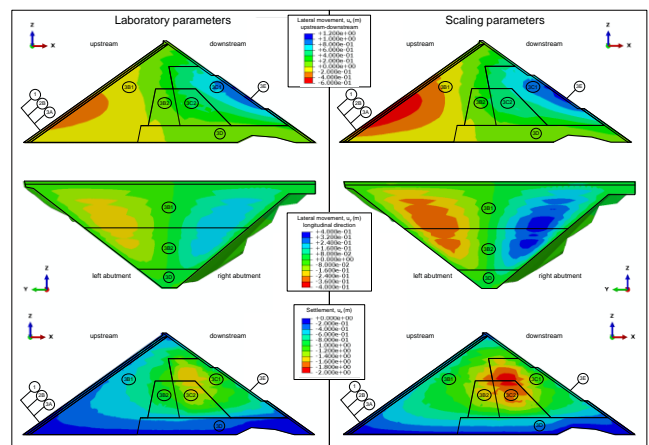


Fig. 13 Contours of the computed dam deformations

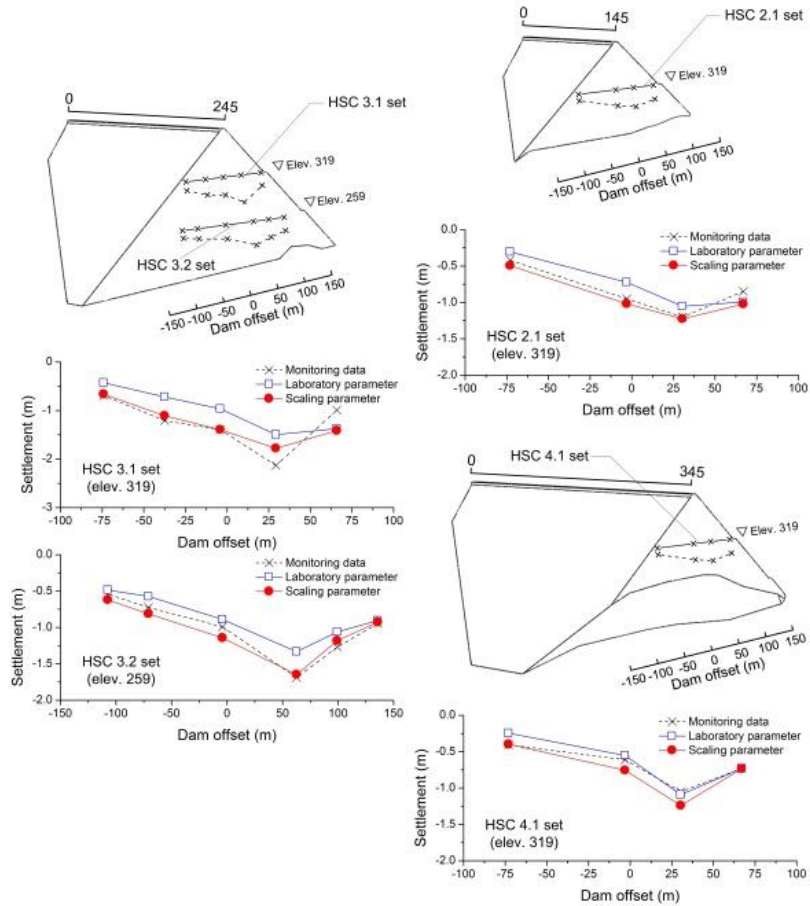
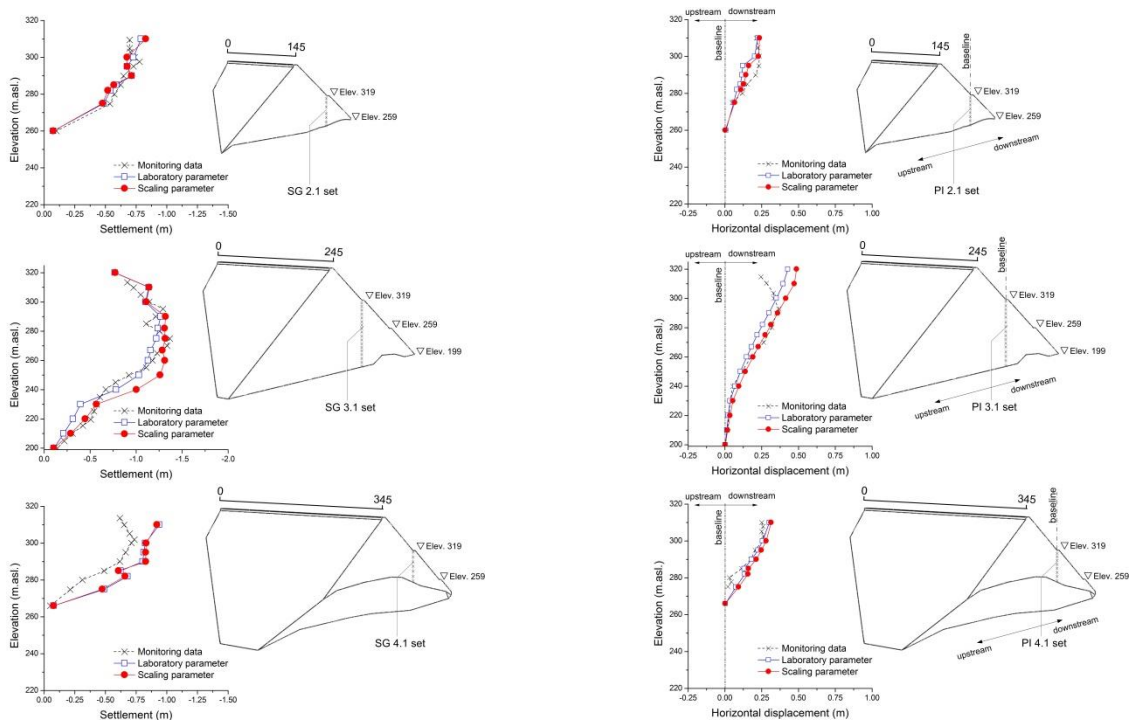


Fig. 14 Comparison of dam settlements from the measurements using HSC and analyses



(a) Comparison of dam settlements from the measurements using SG and analyses

(b) Comparison of dam horizontal displacement (upstream-downstream direction) from the measurements using PI and analyses

Fig. 15 Comparison of dam deformation from the measurements and analyses

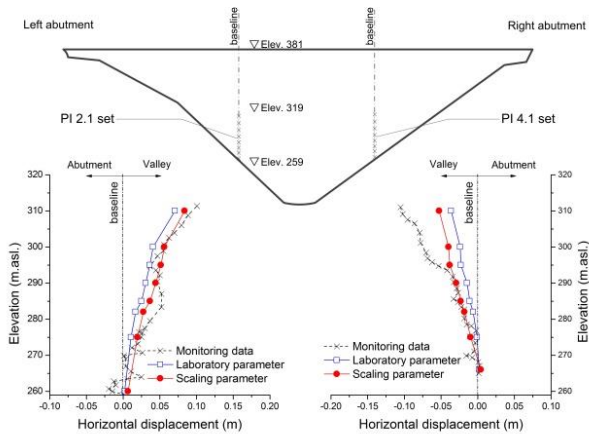


Fig. 16 Comparison of dam horizontal displacement (longitudinal direction) from the measurements and analyses

Fig. 15(b) displays the computed horizontal displacement (upstream-downstream direction) against elevation at various observed sections along with the field monitored data. The monitoring data were obtained from the PI sets. The computed horizontal displacements by SP are generally higher than those by LP. The difference becomes more noticeable at a higher elevation and at a deeper dam section (section 3). The simulation, particularly by SP, can satisfactorily capture the field monitoring data both in the tendency and in the magnitudes, except when the elevation exceeded 290 m for section 3. For sections 2 and 4, both computed results (LP and SP) compare fairly well to the monitoring data. Fig. 16 shows the monitored and computed results of the horizontal displacements along the longitudinal direction. At the left abutment (PI 2.1), the computed results by SP are in generally good agreement with the monitoring data, whereas the results by LP exhibit smaller values. For the right abutment (PI 4.1), the simulation with SP captures the monitoring data well except for when the dam level is higher than 295 m. Like the left abutment case, the computed results by LP are smaller than those by SP. Comparison of the computed results reveals that the deformations predicted from the laboratory parameters are significantly smaller than those from the scaling parameters. Due to the scaling technique used in the tests, the difference between both cases is attributed to the particle size effect. In particular for zones 3B and 3C (main rockfill), the maximum sizes of the materials in actual condition (800 and 1200 mm) are much larger than that prepared in the laboratory (60 mm).

## 9. Conclusions

A method to account for the scaling effects of rockfill materials in rockfill dam deformation analysis was developed based on the modification of material model parameters in numerical simulation. Various sets of experimental data from the literature obtained by varying the particle size and density and a new dataset of Nam Ngum 2 (NN2) rockfill materials obtained by varying the particle gradation were used, and the model parameters

were determined. Simple relations between key influencing factors and model parameters were established to provide the prediction of model parameters from one state to another. Validation by comparing the simulated stress-strain responses between using predicted parameters and the actual testing results was conducted. Moreover, the deformation analyses of NN2 CFRD were carried out by comparing the analysis results with the dam monitoring data to evaluate the performance of the developed method. The following conclusions can be drawn:

- The proposed  $C/F$  concept was proven to be sufficiently suitable to quantitatively take account of the influence of particle gradation of the rockfill materials.
- By comparing with the test data, the proposed method can be effectively used to predict the parameters for simulating the  $q-\varepsilon_a-\varepsilon_v$  response of rockfill materials considering scaling effects.
- Comparisons between the computed dam deformations (by both laboratory and scaling parameter sets) and monitored data showed that by taking account of the scaling effect into model parameter modification using the developed method, the dam deformation prediction by numerical analysis can be fairly improved. Consequently, this proposed method was able to predict the deformation behavior of rockfill dam.

However, the proposed method is based on limited available testing data, particularly the interaction among the influencing parameters. Broader set of laboratory investigations are needed to enhance the efficiency of the method.

## Acknowledgments

This research was funded by Department of Civil Engineering, King Mongkut's University of Technology Thonburi under Contract no. CE-KMUTT 6101 and King Mongkut's University of Technology North Bangkok under Contract no. KMUTNB-60-ART-010. The authors also extend their appreciation to the Thailand Research fund (TRF) through the Royal Golden Jubilee Ph.D. program, under contract grant PHD/0006/2556. They are also indebted to the CK Power Public Company Limited and Nam Ngum 2 Power Company Limited for providing the valuable data.

## References

- Chen, J.F., Liu, J.X., Xue, J.F. and Shi, Z.M. (2014), "Stability analyses of a reinforced soil wall on soft soils using strength reduction method", *Eng. Geol.*, **177**, 83-92.
- Cooke, J.B. (1984), "Progress in rock-fill dams, (18th Terzaghi Lecture)", *J. Geotech. Eng.*, **110**(10), 1381-1414.
- Desai, C.S. (1995), *Constitutive Modeling Using the Disturbed State as Microstructure Self-Adjustment Concept, Continuum Models for Materials with Microstructure*, Wiley, Chichester, U.K.
- Desai, C.S. (2001), *Mechanics of Materials and Interfaces: The Disturbed State Concept*, CRC Press, Boca Raton, Florida, U.S.A.
- Duncan, J.M. and Chang, C.Y. (1970), "Nonlinear analysis of stress-strain in soils", *J. Soil Mech. Found. Div.*, **96**(5), 1629-

- 1653.
- Hamidi, A., Azini, E. and Masoudi, B. (2012), "Impact of gradation on the shear strength-dilation behavior of well graded sand-gravel mixtures", *Sci. Iran.*, **19**(3), 393-402.
- Honkanadavar, N. and Sharma, K. (2014), "Testing and Modeling the Behavior of Riverbed and Blasted Quarried Rockfill Materials", *J. Geomech.*, **14**(6), 04014028.
- Hosseinzadeh, S. and Joosse, J.F. (2015), "Design optimisation of retaining walls in narrow trenches using both analytical and numerical methods", *Comput. Geotech.*, **68**, 338-351.
- ICOLD (2004), *Concrete Face Rockfill Dams: Concepts for Design and Construction 2004*, International Commission on Large Dams, Paris, France.
- IWHR (2007), *Report on Laboratory Tests of the Rockfill Materials of Nam Ngum 2 CFRD*, Institute of Water Resources and Hydropower Research, Beijing, China.
- Jamsawang, P., Yoobanpot, N., Thanasisathit, N., Voottipruex, P. and Jongpradist, P. (2016), "Three-dimensional numerical analysis of a DCM column-supported highway embankment", *Comput. Geotech.*, **72**, 42-46.
- Jia, Y. and Chi, S. (2015), "Back-analysis of soil parameters of the Malutang II concrete face rockfill dam using parallel mutation particle swarm optimization", *Comput. Geotech.*, **65**, 87-96.
- Jongpradist, P., Kaewsri, T., Sawatparnich, A., Suwansawat, S., Youwai, S., Kongkitkul, W. and Sunitsakul, J. (2013), "Development of tunneling influence zones for adjacent pile foundations by numerical analyses", *Tunnell. Undergr. Sp. Technol.*, **34**, 96-109.
- Kang, F., Jun, J.L. and Xu, Q. (2009), "Hybrid simplex artificial bee colony algorithm and its application in material dynamic parameter back analysis of concrete dams", *Shuli Xuebao J. Hydraul. Eng.*, **40**(6), 736-742.
- Kim, Y.S., Seo, M.W., Lee, C.W. and Kang, G.C. (2014), "Deformation characteristics during construction and after impoundment of the CFRD-type Daegok Dam, Korea", *Eng. Geol.*, **178**, 1-14.
- Kokusho, T., Hara, T. and Hiraoka, R. (2004), "Undrained shear strength of granular soils with different particle gradations", *J. Geotech. Geoenviron. Eng.*, **130**(6), 621-629.
- Li, S., Yu, S., Shangguan, Z. and Wang, Z. (2016), "Estimating model parameters of rockfill materials based on genetic algorithm and strain measurements", *Geomech. Eng.*, **10**(1), 37-48.
- Liu, H. and Zou, D. (2013), "Associated generalized plasticity framework for modeling gravelly soils considering particle breakage", *J. Eng. Mech.*, **139**(5), 606-615.
- Lowe, J. (1964), "Shear strength of coarse embankment dam materials", *Proceedings of the 8th International Congress on Large Dams*, Edinburgh, Scotland, May.
- Ma, G., Chang, X.L., Zhou, W. and Ng, T.T. (2014), "Mechanical response of rockfills in a simulated true triaxial test: A combined FDEM study", *Geomech. Eng.*, **7**(3), 317-333.
- Marachi, N.D., Chan, C.K., Seed, H.B. and Duncan, J.M. (1969), *Strength and Deformation Characteristics of Rockfill Materials*, Rep. No. TE 69-5, Civil Engineering Department, University of California, Berkeley, California, U.S.A.
- Marsal, R.J. (1967), "Large Scale Testing of Rockfill Materials", *J. Soil Mech. Found. Div.*, **93**(SM2), 27-43.
- Meng, F., Zhang, J.S., Chen, X.B. and Wang, Q.Y. (2014), "Deformation characteristics of coarse-grained soil with various gradations", *J. Central South Univ.*, **21**(6), 2469-2476.
- Mroz, Z. and Zienkiewicz, O.C. (1984), *Uniform formulation of Constitutive Equations for Clay and Sand*, in *Mechanics of engineering materials*, John Wiley and Sons, Chichester, England.
- NJHRI. (1999), "Specification of soil test (SL 237-1999)", Ministry of Water Resources of the People's Republic of China, China Water Resources and Hydropower Press, Beijing.
- Pramthawee, P., Jongpradist, P. and Kongkitkul, W. (2011), "Evaluation of hardening soil model on numerical simulation of behaviors of high rockfill dams", *Songklanakarinn J. Sci. Technol.*, **33**(3), 325-334.
- Pramthawee, P., Jongpradist, P. and Sukkarak, R. (2017), "Integration of creep into a modified hardening soil model for time-dependent analysis of a high rockfill dam", *Comput. Geotech.*, **91**, 104-116.
- Ramon, A., Romero, E.E. and Alonso, E.E. (2008), "Grain size effects on rockfill constitutive behaviour", *Proceedings of the 1st European Conference on Unsaturated Soils*, Durham, U.K., July.
- Rowe, P.W. (1962), "The stress-dilatancy relation for static equilibrium of an assembly of particles in contact", *Proc. Royal Soc. A.*, **269**, 500-527.
- Sánchez-Leal, F. (2007), "Gradation Chart for Asphalt Mixes: Development", *J. Mater. Civ. Eng.*, **19**(2), 185-197.
- Schanz, T., Vermeer, P.A. and Bonnier, P.G. (1999), *The Hardening Soil Model-Formulation and Verification*, in *Beyond 2000 in Computational Geotechnics*, Balkema, Amsterdam, Rotterdam, The Netherlands.
- Sukkarak, R., Pramthawee, P. and Jongpradist, P. (2017), "A Modified Elasto-plastic model with double yield surfaces and considering particle breakage for the settlement analysis of high rockfill dams", *KSCE J. Civ. Eng.*, **21**(3), 734-745.
- Tabibnejad, A., Heshmati, A., Salehzadeh, H. and Tabatabaei, S.H. (2014), "Effect of gradation curve and dry density on collapse deformation behavior of a rockfill material", *KSCE J. Civ. Eng.*, **19**(3), 631-640.
- Tunsakul, J., Jongpradist, P., Kongkitkul, W., Wonglert, A. and Youwai, S. (2013), "Investigation of failure behavior of continuous rock mass around cavern under high internal pressure", *Tunnell. Undergr. Sp. Technol.*, **34**, 110-123.
- Varadarajan, A., Sharma, K., Venkatachalam, K. and Gupta, A. (2003), "Testing and modeling two rockfill materials", *J. Geotech. Geoenviron.*, **129**(3), 206-218.
- Varadarajan, A., Sharma, K.G., Abbas, S.M. and Dhawan, A.K. (2006), "Constitutive model for rockfill materials and determination of material constants", *J. Geomech.*, **6**(4), 226-237.
- Wang, Z., Liu, S., Vallejo, L. and Wand, L. (2014), "Numerical analysis of the causes of face slab cracks in Gongboxia rockfill dam", *Eng. Geol.*, **181**, 224-232.
- Wei, K.M., Zhu, S.H. and Yu, X.H. (2014), "Influence of the scale effect on the mechanical parameters of coarse-grained soils", *Iran. J. Sci. Technol. Trans. Civ. Eng.*, **38**(C1), 75-84.
- Xiao, Y., Liu, H., Chen, Y. and Jiang, J. (2014), "Strength and deformation of rockfill material based on large-scale triaxial compression tests. I: Influences of density and pressure", *J. Geotech. Geoenviron.*, **14**(12), 04014070.
- Xu, B., Zou, J. and Liu, H. (2012b), "Three-dimensional simulation of the construction process of the Zipingpu concrete face rockfill dam based on a generalized plasticity model", *Comput. Geotech.*, **43**, 143-154.
- Xu, M., Song, E. and Chen, J. (2012a), "A large triaxial investigation of the stress-path-dependent behavior of compacted rockfill", *Acta. Geotech.*, **7**(3), 167-175.
- Yu, S.Z., Jie, L.J. and Yu, W.H. (2007), "Inverse research for gravity dam parameters based on chaos artificial fish swarm algorithm", *Yantu Lixue Rock Soil Mech.*, **28**(10), 2193-2196.
- Zhang, G. and Zhang, J.M. (2008), "Unified modeling of monotonic and cyclic behavior of interface between structure and gravelly soil", *Soil. Found.*, **48**(2), 231-245.
- Zhang, G., Zhang, J.M. and Yu, Y. (2007), "Modeling of Gravelly Soil with Multiple Lithologic Components and its Application", *Soil. Found.*, **47**(4), 799-810.

- Zheng, D., Cheng, L., Bao, T. and Lv, B. (2013), "Integrated parameter inversion analysis method of a CFRD based on multi-output support vector machines and the clonal selection algorithm", *Comput. Geotech.*, **47**, 68-77.
- Zhou, W., Hua, J., Chang, X. and Zhou, C. (2011), "Settlement analysis of the Shuibuya concrete-face rockfill dam", *Comput. Geotech.*, **38**(2), 269-280.
- Zhou, W., Li, S.L., Ma, G., Chang, X.L., Cheng, Y.G. and Ma, X. (2016), "Assessment of the crest cracks of the Pubugou rockfill dam based on parameters back analysis", *Geomech. Eng.*, **11**(4), 571-585.